

Phase Behavior of the System Linear Polyglycerol + Methanol + Carbon Dioxide

Christian S. Schacht,[†] Christoph Schuell,[‡] Holger Frey,[‡] Theo W. de Loos,[†] and Joachim Gross^{*,†,§}

[†]Engineering Thermodynamics, Process and Energy Department, Delft University of Technology, Delft, The Netherlands

[‡]Institute of Organic Chemistry, Johannes Gutenberg-University Mainz, Mainz, Germany

[§]Institute of Thermodynamics and Thermal Process Engineering, University of Stuttgart, Stuttgart, Germany

ABSTRACT: To compare the phase behavior of linear and hyperbranched polymers, the phase envelopes of the ternary system linear polyglycerol + methanol + carbon dioxide were determined for polymers of varying molar mass. Phase changes were detected by a static synthetic method using the Cailletet setup for temperatures between 331 K and 421 K and pressures up to 13.1 MPa. Besides the vapor–liquid and liquid–liquid equilibria, also the vapor–liquid to vapor–liquid–liquid and vapor–liquid–liquid to liquid–liquid phase boundaries are reported. The experimental results are similar to systems with hyperbranched polymers (rather than linear polymers). For the systems with linear polymers, however, the bubble-point pressures show no significant dependence on the polymer molar mass, whereas for hyperbranched polymers the bubble-point pressure was found to vary substantially with the polymer molecular mass. Further, the polymer concentration at the lower critical solution temperature is remarkably high when the polymers have a hyperbranched structure (Schacht et al., *Fluid Phase Equilib.* **2010**, *299*, 252–258), while the polymer concentration is much lower for systems with linear polymers.

INTRODUCTION

According to Flory and Huggins' theory, the solvent activity coefficient of a typical polymer solution converges toward a minimum with an increasing size difference of polymer and solvent at a constant temperature and composition.^{1,2} These mixtures exhibit a constant bubble-point pressure upon reaching sufficiently high molar masses at a given temperature and composition.^{3,4} In contrast, it was shown that the bubble-point pressures for mixtures of hyperbranched polyglycerol⁵ + methanol + carbon dioxide changes significantly with the polymer molar mass.⁶ Seemingly, the phase behavior of the hyperbranched polyglycerol system deviates from the Flory–Huggins theory. This suggests that a structural effect, for example, the crowding of functional groups in the shell of the polyglycerol molecule, causes the polymer size dependency of the bubble-point pressure in these systems. To substantiate this finding, we here determine the vapor–liquid equilibria of the system linear polyglycerol (IPG) + methanol + carbon dioxide at varying polymer molar masses. These linear polyglycerols have approximately the same molecular composition as the hyperbranched polyglycerols used in the earlier investigations.⁶ The comparison of the two different systems then allows a direct comparison of how the linear and hyperbranched polymer structures influence the phase behavior of polymer–solvent mixtures.

MATERIALS AND EXPERIMENTAL METHODS

The carbon dioxide used in this work was obtained from Hoek Loos with a minimum purity of $w_{\text{CO}_2} = 0.99995$, and methanol with a purity of $w_{\text{MeOH}} = 0.985$ was purchased from J.T. Baker, where w_i is the mass fraction of compound i . α -(1,1-Dimethylethyl)- ω -hydropoly[oxy(1-hydroxymethyl)ethylene], more commonly known as linear polyglycerol, with a number

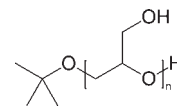


Figure 1. Chemical structure of linear polyglycerol.

based molar mass of $M_n = 3.9$ ($M_w/M_n = 1.4$), $M_n = 4.8$ ($M_w/M_n = 1.2$), and $M_n = 7.8 \text{ kg} \cdot \text{mol}^{-1}$ ($M_w/M_n = 1.3$) was used in this work. The synthesis was performed according to literature procedures^{7,8} using potassium *tert*-butanolate as the initiator and ethoxy ethyl glycidyl ether (EEGE) as a monomer to yield linear polyglycerol after the removal of the protection groups under acidic conditions. The molar mass distributions as well as the polydispersities (M_w/M_n) have been determined by size exclusion chromatography using polystyrene standards. The structure of the polymer is shown in Figure 1. Prior to sample preparation the polymer was kept in a vacuum oven at 80 °C to reduce the water content to a minimum. Mixtures of methanol and polyglycerol were prepared and degassed by repeated freezing and melting under vacuum. Carbon dioxide was added by a gas volumetric method. The size of a typical sample was 0.1 g with uncertainties of less than $\pm 0.0001 \text{ g}$ for each component. The water content of all samples was determined by Karl Fischer titration and is given in Table 1. The mixtures' isopleths were determined by a static-synthetic method using the Cailletet apparatus. A detailed description of the experimental setup can be found elsewhere.⁹ Using this method, phase changes can be determined visually by pressure adjustments at constant temperature. Pressures are measured with a dead weight gauge at an

Received: February 14, 2011

Accepted: May 4, 2011

Published: May 11, 2011

accuracy of ± 0.005 MPa. Temperature measurements are taken with a platinum resistance thermometer at an accuracy of ± 0.02 K.

Table 1. Water Content $w_{\text{H}_2\text{O}}$ (Mass Fraction) of the Samples

system ^a	$w_{\text{H}_2\text{O}}$
[0.499 IPG ($3.9 \text{ kg}\cdot\text{mol}^{-1}$) + 0.501 CH_3OH]	0.0021
[0.250 IPG ($3.9 \text{ kg}\cdot\text{mol}^{-1}$) + 0.750 CH_3OH]	0.0011
[0.501 IPG ($4.8 \text{ kg}\cdot\text{mol}^{-1}$) + 0.499 CH_3OH]	0.0022
[0.250 IPG ($4.8 \text{ kg}\cdot\text{mol}^{-1}$) + 0.750 CH_3OH]	0.0007
[0.501 IPG ($7.8 \text{ kg}\cdot\text{mol}^{-1}$) + 0.499 CH_3OH]	0.0019
[0.250 IPG ($7.8 \text{ kg}\cdot\text{mol}^{-1}$) + 0.750 CH_3OH]	0.0010

^a Numbers indicate mass fractions.

Table 2. Experimental Bubble-Point Pressures p for $w_1 \text{ CO}_2 + (1 - w_1) [w_2 \text{ IPG } (3.9 \text{ kg}\cdot\text{mol}^{-1}) + w_3 \text{ CH}_3\text{OH}]$ at Given Temperature T , where w_i is the Mass Fraction of Compound i ^a

$w_2 = 0.499, w_3 = 0.501$				$w_2 = 0.250, w_3 = 0.750$			
$w_1 = 0.053$		$w_1 = 0.105$		$w_1 = 0.050$		$w_1 = 0.100$	
T/K	p/MPa	T/K	p/MPa	T/K	p/MPa	T/K	p/MPa
333.16	2.412	331.53	4.382	333.03	1.579	331.59	2.948
343.12	2.755	341.46	5.042	343.06	1.797	341.56	3.340
353.00	3.122	351.47	5.722	353.09	2.030	351.55	3.748
363.04	3.512	361.43	6.418	363.15	2.280	361.54	4.166
373.11	3.913	371.43	7.133	373.22	2.555	371.58	4.599
383.08	4.348	381.35	7.866	383.23	2.838	381.52	5.042
393.10	4.798	391.29	8.602	393.21	3.156	391.51	5.500
403.09	5.286	401.22	9.353	403.09	3.499	401.48	5.968
				413.09	3.864	411.46	6.458
				423.02	4.289	421.17	6.959

^a $u(T) = 0.02$ K, $u(p) = 0.005$ MPa, and $u(w_1) = u(w_2) = u(w_3) = 0.001$.

Table 3. Experimental Data for the Bubble Point (gl), Cloud Point (ll), Phase Boundary Vapor–Liquid to Liquid–Liquid–Vapor (gll), and the Phase Boundary Liquid–Liquid–Vapor to Liquid–Liquid (lgl) for $w_1 \text{ CO}_2 + (1 - w_1) [w_2 \text{ IPG } (4.8 \text{ kg}\cdot\text{mol}^{-1}) + w_3 \text{ CH}_3\text{OH}]$, where w_i is the Mass Fraction of Compound i , T the Temperature, and p the Pressure^a

$w_2 = 0.501, w_3 = 0.499$				$w_2 = 0.250, w_3 = 0.750$			
$w_1 = 0.052$		$w_1 = 0.100$		$w_1 = 0.050$		$w_1 = 0.100$	
T/K	p/MPa	T/K	p/MPa	T/K	p/MPa	T/K	p/MPa
333.12	2.430 (gl)	331.74	4.537 (gl)	333.04	1.403 (gl)	331.68	2.748 (gl)
343.10	2.790 (gl)	341.70	5.258 (gl)	343.03	1.614 (gl)	341.66	3.131 (gl)
353.04	3.181 (gl)	351.68	5.944 (gl)	353.07	1.839 (gl)	351.65	3.541 (gl)
363.03	3.581 (gl)	361.64	6.682 (gl)	363.12	2.096 (gl)	361.76	3.957 (gl)
373.04	3.999 (gl)	371.63	7.432 (gl)	373.15	2.364 (gl)	371.62	4.382 (gl)
383.01	4.442 (gl)	381.56	8.200 (gl)	383.13	2.654 (gl)	381.67	4.825 (gl)
393.00	4.907 (gl)	391.19	8.976 (gl)	393.11	2.965 (gl)	391.31	5.283 (gl)
403.01	5.408 (gl)	401.13	9.776 (gl)	403.10	3.305 (gl)	401.27	5.751 (gl)
412.98	5.943 (gl)	406.15	9.778 (gll)	413.05	3.681 (gl)	411.25	6.234 (gl)
422.99	6.517 (gl)	411.08	9.916 (gll)	423.02	4.101 (gl)	421.23	6.744 (gl)
		406.15	10.100 (lgl)				
		411.08	10.391 (lgl)				
		406.15	11.026 (ll)				
		411.08	12.462 (ll)				

^a $u(T) = 0.02$ K, $u(p) = 0.005$ MPa, and $u(w_1) = u(w_2) = u(w_3) = 0.001$.

Silicone oil served as the thermostat liquid, and the temperature could be kept in a range of ± 0.02 K by PID control.

RESULTS AND DISCUSSION

Vapor–liquid phase equilibria were determined for systems of linear polyglycerol + methanol + carbon dioxide. A target of this study is the evaluation and comparison of how the molar mass of linear and of hyperbranched polymers affect the phase behavior. Mixtures with linear polyglycerol of $M_n = 3.9 \text{ kg}\cdot\text{mol}^{-1}$, $M_n = 4.8 \text{ kg}\cdot\text{mol}^{-1}$, and $M_n = 7.8 \text{ kg}\cdot\text{mol}^{-1}$ were investigated at different ratios of methanol to polyglycerol and for two carbon dioxide concentrations. The experimental results are given in Tables 2 to 4. The pressure–temperature phase envelopes for these systems are given in Figures 2 to 5. As can be seen in Figure 2, the water concentration has a significant influence on the phase behavior of these mixtures. In the following only systems with approximately the same water content are compared.

Figure 3 shows the increasing bubble-point pressure for the system linear polyglycerol ($M_n = 3.9 \text{ kg}\cdot\text{mol}^{-1}$) + methanol + carbon dioxide with increasing carbon dioxide concentrations. Increasing methanol concentrations, on the other hand, result in decreased bubble-point pressures and, thus, in higher carbon dioxide solubilities. For mixtures of polymers with higher molar mass ($M_n = 4.8 \text{ kg}\cdot\text{mol}^{-1}$ and $7.8 \text{ kg}\cdot\text{mol}^{-1}$), in Figures 4 and 5, one can observe the formation of a liquid–liquid–vapor region with lower solution temperature (LST) due to the demixing of the liquid phase at higher temperatures. The demixing is a result of the reduced entropy of mixing caused by the different expansivities of methanol and polyglycerol at higher temperatures. The addition of carbon dioxide reduces the solvent power of methanol and shifts the LST to lower temperatures and higher pressures. This behavior is in accordance with other systems in literature.^{10,11} Increasing the methanol concentrations or the polymer molar mass results in decreased LSTs. It could further be

Table 4. Experimental Data for the Bubble Point (gl), Cloud Point (ll), Phase Boundary Vapor–Liquid to Liquid–Liquid–Vapor (gll), and Phase Boundary Liquid–Liquid–Vapor to Liquid–Liquid (lgl) for w_1 CO₂ + (1 - w_1) [w_2 IPG (7.8 kg·mol⁻¹) + w_3 CH₃OH], where w_i is the Mass Fraction of Compound i , T the Temperature, and p the Pressure^a

$w_2 = 0.501, w_3 = 0.499$				$w_2 = 0.250, w_3 = 0.750$			
$w_1 = 0.050$		$w_1 = 0.100$		$w_1 = 0.050$		$w_1 = 0.100$	
T/K	p/MPa	T/K	p/MPa	T/K	p/MPa	T/K	p/MPa
333.12	2.391 (gl)	331.75	4.243 (gl)	333.07	1.480 (gl)	331.83	2.694 (gl)
353.07	3.082 (gl)	341.40	4.884 (gl)	343.04	1.697 (gl)	341.68	3.077 (gl)
363.07	3.467 (gl)	351.71	5.559 (gl)	353.02	1.930 (gl)	351.62	3.485 (gl)
373.05	3.858 (gl)	361.63	6.245 (gl)	362.97	2.173 (gl)	361.59	3.903 (gl)
383.06	4.257 (gl)	371.61	6.945 (gl)	372.97	2.441 (gl)	371.56	4.336 (gl)
393.04	4.708 (gl)	381.56	7.660 (gl)	382.96	2.731 (gl)	381.51	4.778 (gl)
403.04	5.182 (gl)	391.19	8.286 (gl)	392.97	3.041 (gl)	391.48	5.236 (gl)
413.04	5.693 (gl)	401.13	8.406 (gl)	402.99	3.382 (gl)	401.44	5.712 (gl)
423.01	6.244 (gl)	406.27	8.436 (gl)	412.97	3.757 (gl)	411.45	6.197 (gl)
		391.43	8.386 (lgl)	422.96	4.202 (gl)	416.37	6.157 (gl)
		401.34	8.979 (lgl)			421.41	6.045 (gl)
		406.27	9.261 (lgl)			416.37	6.440 (lgl)
		401.34	11.383 (ll)			421.41	6.662 (lgl)
		406.27	13.083 (ll)			416.37	7.145 (ll)
						421.41	8.796 (ll)

^a $u(T) = 0.02$ K, $u(p) = 0.005$ MPa, and $u(w_1) = u(w_2) = u(w_3) = 0.001$.

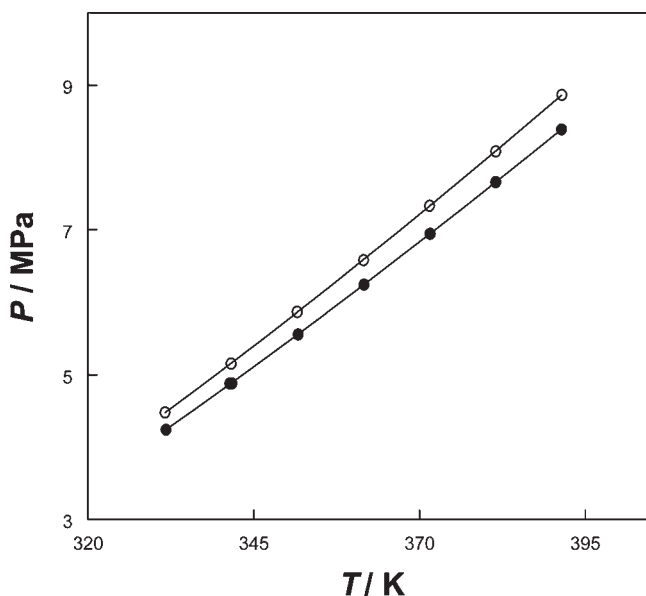


Figure 2. Comparison of the bubble-point curves of the ternary system (1 - w_{CO_2}) [0.5 IPG ($M_n = 7.8$ kg·mol⁻¹) + 0.5 methanol] + CO₂ with $w_{CO_2} = 0.1$ at different water contents of $w_{H_2O} = 0.0043$ (open circles) and $w_{H_2O} = 0.0019$ (solid circles). The lines are polynomial fits to the data.

observed, that the polymer concentration at the lower critical solution temperature is lower than $w_{polymer} = 0.25$ for all systems investigated. This has also been reported for other solutions with linear polymers¹² and deviates from the findings for systems including hyperbranched polyglycerols.⁶ For these systems polymer concentrations at the lower critical solution temperature were exceeding $w_{polymer} = 0.5$.

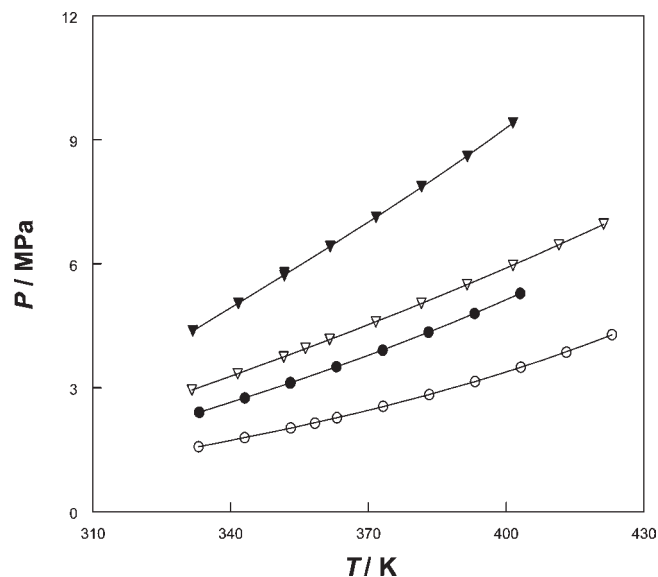


Figure 3. Influence of polymer concentration on the phase behavior of linear polyglycerol (IPG) ($M_n = 3.9$ kg·mol⁻¹) + methanol + CO₂, with $w_{CO_2} = 0.05$ (circles) and $w_{CO_2} = 0.1$ (triangles). The open symbols are for w_{CO_2} CO₂ + (1 - w_{CO_2}) [0.25 IPG + 0.75 methanol], and the closed symbols are for w_{CO_2} CO₂ + (1 - w_{CO_2}) [0.5 IPG + 0.5 methanol]. The lines are polynomial fits to the data.

The systems investigated in this work can be classified as type IV systems according to Van Konynenburg and Scott¹³ (type 2^P1 as recommended by the IUPAC¹⁴), and their phase behavior is similar to the phase behavior of hyperbranched polyglycerol + methanol + carbon dioxide systems, which were determined in earlier works.^{6,15} This is demonstrated in Figure 6 by comparing the bubble- and cloud-point curves of a hyperbranched and a

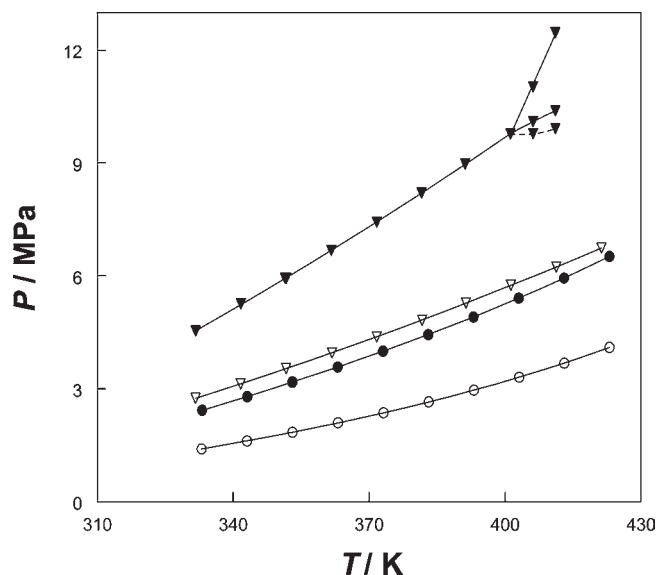


Figure 4. Influence of polymer concentration on the phase behavior of IPG ($M_n = 4.8 \text{ kg}\cdot\text{mol}^{-1}$) + methanol + CO_2 , with $w_{\text{CO}_2} = 0.05$ (circles) and $w_{\text{CO}_2} = 0.1$ (triangles). The open symbols are for $w_{\text{CO}_2} \text{CO}_2 + (1 - w_{\text{CO}_2}) [0.25 \text{ IPG} + 0.75 \text{ methanol}]$, and the closed symbols are for $w_{\text{CO}_2} \text{CO}_2 + (1 - w_{\text{CO}_2}) [0.5 \text{ IPG} + 0.5 \text{ methanol}]$. The lines are polynomial fits to the data.

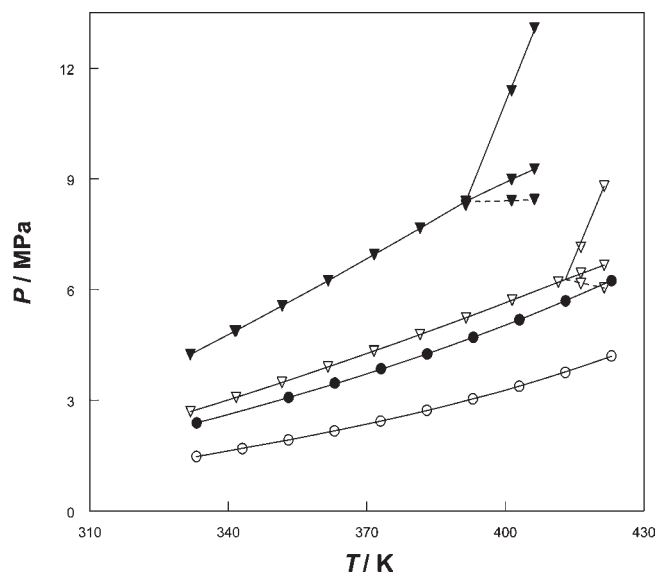


Figure 5. Influence of polymer concentration on the phase behavior of linear polyglycerol (IPG) ($M_n = 7.8 \text{ kg}\cdot\text{mol}^{-1}$) + methanol + CO_2 , with $w_{\text{CO}_2} = 0.05$ (circles) and $w_{\text{CO}_2} = 0.1$ (triangles). The open symbols are for $w_{\text{CO}_2} \text{CO}_2 + (1 - w_{\text{CO}_2}) [0.25 \text{ IPG} + 0.75 \text{ methanol}]$, and the closed symbols are for $w_{\text{CO}_2} \text{CO}_2 + (1 - w_{\text{CO}_2}) [0.5 \text{ IPG} + 0.5 \text{ methanol}]$. The lines are polynomial fits to the data.

linear polyglycerol in mixture with methanol and carbon dioxide. The molar masses of the hyperbranched and the linear polyglycerol are $M_n = 5.7 \text{ kg}\cdot\text{mol}^{-1}$ and $M_n = 4.8 \text{ kg}\cdot\text{mol}^{-1}$, respectively. The dependency of the LST on the methanol concentration is, however, more pronounced in the system containing the hyperbranched polymer. The experimental findings in this work also indicate that the LST is less dependent on

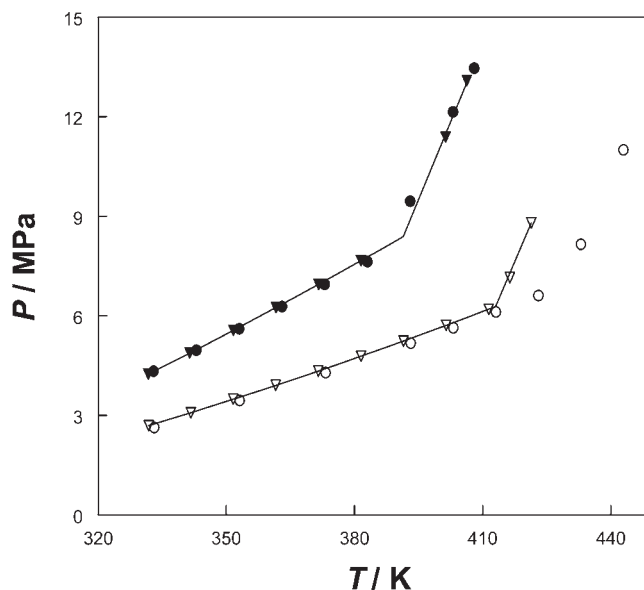


Figure 6. Comparison of the LSTs of hyperbranched (circles) and linear (triangles) polyglycerols (PG). The graph shows experimental bubble-point and cloud-point curves of the ternary systems $(1 - w_{\text{CO}_2}) [0.5 \text{ PG} + 0.5 \text{ methanol}] + \text{CO}_2$ (solid symbols) and $(1 - w_{\text{CO}_2}) [0.25 \text{ PG} + 0.75 \text{ methanol}] + \text{CO}_2$ (open symbols), with $w_{\text{CO}_2} = 0.1$. The molar masses of the linear and hyperbranched polyglycerols are $M_n = 7.8 \text{ kg}\cdot\text{mol}^{-1}$ and $M_n = 5.7 \text{ kg}\cdot\text{mol}^{-1}$, respectively. Data for the hyperbranched polyglycerol system are taken from ref 6. The lines are polynomial fits to the data.

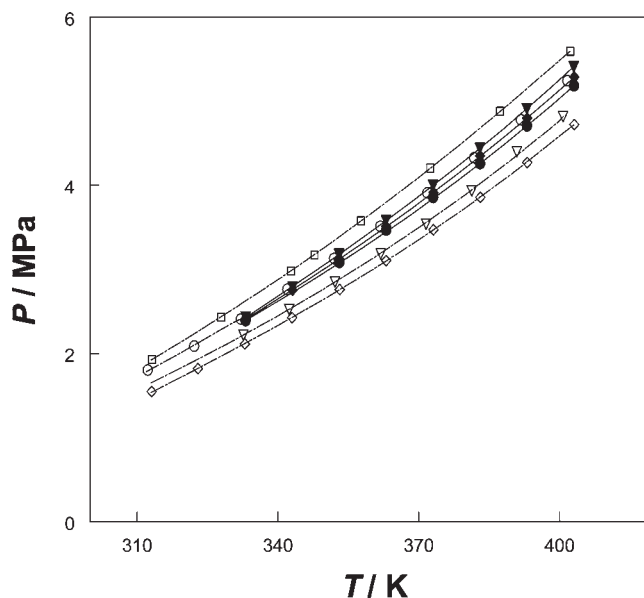


Figure 7. Bubble-point curves of the ternary systems $(1 - w_{\text{CO}_2}) [0.5 \text{ hyperbranched PG} + 0.5 \text{ methanol}] + \text{CO}_2$ (open symbols) and $(1 - w_{\text{CO}_2}) [0.5 \text{ linear PG} + 0.5 \text{ methanol}] + \text{CO}_2$, with $w_{\text{CO}_2} = 0.05$. The molar mass of the hyperbranched PG is varying; $M_n = 2.7 \text{ kg}\cdot\text{mol}^{-1}$ (open diamonds), $M_n = 5.7 \text{ kg}\cdot\text{mol}^{-1}$ (open triangles), $M_n = 10 \text{ kg}\cdot\text{mol}^{-1}$ (open circles), and $M_n = 18 \text{ kg}\cdot\text{mol}^{-1}$ (open squares). Data for $M_n = 2.7 \text{ kg}\cdot\text{mol}^{-1}$ are taken from ref 15, and data for $M_n = 5.7 \text{ kg}\cdot\text{mol}^{-1}$, $M_n = 10 \text{ kg}\cdot\text{mol}^{-1}$, and $M_n = 18 \text{ kg}\cdot\text{mol}^{-1}$ are taken from ref 6. The molar mass of the linear polyglycerol is $M_n = 3.9 \text{ kg}\cdot\text{mol}^{-1}$ (solid diamonds), $M_n = 4.8 \text{ kg}\cdot\text{mol}^{-1}$ (solid triangles), and $M_n = 7.8 \text{ kg}\cdot\text{mol}^{-1}$ (solid circles), respectively. The lines are polynomial fits to the data.

the polymer molar mass than for comparable systems with hyperbranched polymers.

A comparison of the bubble-point pressure of the system polyglycerol + methanol + carbon dioxide with hyperbranched and linear polyglycerols at increasing molar masses is shown in Figure 7. The molar mass has almost no influence on the vapor–liquid phase boundary of the system including linear polyglycerol. This finding is in agreement with the Flory–Huggins theory, which states that the solvent activity coefficient in an athermal polymer solution becomes independent of the polymer size at high enough polymer molar masses.¹ For linear polyglycerol + methanol mixtures the activity coefficient can be estimated from the Flory–Huggins expression.² At polymer molar masses above $M_n = 3.0 \text{ kg} \cdot \text{mol}^{-1}$ the activity coefficient does not change significantly with increasing molar mass. We conclude that the dependence of bubble-point pressures on the molar mass of hyperbranched polymers, as described earlier⁶ and shown in Figure 7, can be related to the molecular structure of the polymer.

The differences in bubble-point pressures for the linear polyglycerol systems of increasing molar mass can be explained by the slight variations of carbon dioxide concentration (for the exact concentrations compare Tables 2 to 4) and water content in these samples.

CONCLUSIONS

A systematic analysis of the impact of polymer molar mass on the phase behavior of linear polyglycerol + carbon dioxide + methanol mixtures is presented. The phase behavior of these mixtures can be identified as a type IV system according to the classification of Van Konynenburg and Scott.¹³ The experimental results are similar to the phase behavior for systems of hyperbranched polyglycerols + methanol + carbon dioxide.⁶ However, two aspects are different. First, in contrast to the systems including hyperbranched polymers, the bubble-point pressures for the systems with linear polymers did not change with increasing polymer molar mass in the present investigation. It can, thus, be concluded that the dependence of the bubble-point pressure on the polymer size is due to the branched structure of the hyperbranched polyglycerol. This behavior is not yet captured by statistically based thermodynamic models and encourages their further development. Second, the exceptionally high polymer concentration at the lower critical solution temperature could only be found in systems with hyperbranched polyglycerol⁶ and, therefore, forms a characteristic trait of phase equilibria including dendritic compounds.

AUTHOR INFORMATION

Corresponding Author

*E-mail: gross@itt.uni-stuttgart.de.

Funding Sources

The financial support of Shell Global Solutions (Amsterdam) is appreciated.

ACKNOWLEDGMENT

The authors would like to thank Eugene Straver for his assistance with the experimental work.

REFERENCES

- (1) Prausnitz, J. M.; Lichtenthaler, R. N.; Gomes de Azevedo, E. *Molecular thermodynamics of fluid-phase equilibria*, 3rd ed.; Prentice Hall PTR: Upper Saddle River, NJ, 1999.
- (2) Flory, P. I. Thermodynamics of high polymer solutions. *J. Chem. Phys.* **1942**, *10*, 51–61.
- (3) Weidner, E.; Wiesmet, V.; Knez, Z.; Skerget, M. Phase equilibrium (solid-liquid-gas) in polyethyleneglycol-carbon dioxide systems. *J. Supercrit. Fluids* **1997**, *10*, 139–147.
- (4) Sato, Y.; Takikawa, T.; Yamane, M.; Takishima, S.; Masuoka, H. Solubility of carbon dioxide in PPO and PPO/PS blends. *Fluid Phase Equilib.* **2002**, *194*, 847–858.
- (5) Wilms, D.; Stiriba, S. E.; Frey, H. Hyperbranched polyglycerols: From the controlled synthesis of biocompatible polyether polyols to multipurpose applications. *Acc. Chem. Res.* **2010**, *43*, 129–141.
- (6) Schacht, C.; Bahramali, S.; Wilms, D.; Frey, H.; Gross, J.; de Loos, T. Phase behavior of the system hyperbranched polyglycerol + methanol + carbon dioxide. *Fluid Phase Equilib.* **2010**, *299*, 252–258.
- (7) Taton, D.; Leborgne, A.; Sepulchre, M.; Spassky, N. Synthesis of chiral and racemic functional polymers from glycidol and thioglycidol. *Macromol. Chem. Phys.* **1994**, *195*, 139–148.
- (8) Keul, H.; Moller, M. Synthesis and degradation of biomedical materials based on linear and star shaped polyglycidols. *J. Polym. Sci., Part A: Polym. Chem.* **2009**, *47*, 3209–3231.
- (9) De Loos, T. W.; Van der Kooi, H. J.; Ott, P. L. Vapor-liquid critical curve of the system ethane + 2-methylpropane. *J. Chem. Eng. Data* **1986**, *31*, 166–168.
- (10) Ter Horst, M. H.; Behme, S.; Sadowski, G.; De Loos, T. W. The influence of supercritical gases on the phase behavior of polystyrene-cyclohexane and polyethylene-cyclohexane systems: experimental results and modeling with the SAFT-equation of state. *J. Supercrit. Fluids* **2002**, *23*, 181–194.
- (11) Kiran, E.; Zhuang, W. H.; Sen, Y. L. Solubility and demixing of polyethylene in supercritical binary fluid mixtures - carbon-dioxide cyclohexane, carbon-dioxide toluene, carbon-dioxide pentane. *J. Appl. Polym. Sci.* **1993**, *47*, 895–909.
- (12) Vanopstal, L.; Koningsveld, R. Mean-field lattice equations of state: 4. Influence of pressure on the phase-behavior of the system polystyrene cyclohexane. *Polymer* **1992**, *33*, 3433–3444.
- (13) Konynenburg, P. H. V.; Scott, R. L. Critical Lines and Phase Equilibria in Binary Van Der Waals Mixtures. *Philos. Trans. R. Soc. London, Ser. A* **1980**, *298*, 495–540.
- (14) Bolz, A.; Deiters, U. K.; Peters, C. J.; de Loos, T. W. Nomenclature for phase diagrams with particular reference to vapour-liquid and liquid-liquid equilibria (technical report). *Pure Appl. Chem.* **1998**, *70*, 2234–2257.
- (15) Kozłowska, M. K.; Jurgens, B. F.; Schacht, C. S.; Gross, J.; de Loos, T. W. Phase Behavior of Hyperbranched Polymer Systems: Experiments and Application of the Perturbed-Chain Polar SAFT Equation of State. *J. Phys. Chem. B* **2009**, *113*, 1022–1029.